THE UNIVERSITY OF
WARWICK

Original citation:
Hassan, A. H. A., Morris, R. J. H. (Richard J. H.), Mironov, O. A., Beanland, Richard, Walker, David, 1978-, Huband, S., Dobbie, A. (Andrew), Myronov, Maksym and Leadley, D. R. (David R.). (2014) Anisotropy in the hole mobility measured along the [110] and [1¯10] orientations in a strained Ge quantum well. Applied Physics Letters, Volume 104 (Number 13). Article number 132108. ISSN 0003-6951

Permanent WRAP url:
http://wrap.warwick.ac.uk/60425

Copyright and reuse:
The Warwick Research Archive Portal (WRAP) makes this work of researchers of the University of Warwick available open access under the following conditions.

This article is made available under the Creative Commons Attribution 3.0 (CC BY 3.0) license and may be reused according to the conditions of the license. For more details see: http://creativecommons.org/licenses/by/3.0/

A note on versions:
The version presented in WRAP is the published version, or, version of record, and may be cited as it appears here.

For more information, please contact the WRAP Team at: publications@warwick.ac.uk

http://wrap.warwick.ac.uk

APPLIED PHYSICS LETTERS **104**, 132108 (2014)

Anisotropy in the hole mobility measured along the [110] and [$\bar{1}$10] orientations in a strained Ge quantum well

A. H. A. Hassan,[a)] R. J. H. Morris, O. A. Mironov,[b)] R. Beanland, D. Walker, S. Huband, A. Dobbie, M. Myronov, and D. R. Leadley
Department of Physics, University of Warwick Coventry, Coventry CV4 7AL, United Kingdom

(Received 9 January 2014; accepted 3 March 2014; published online 2 April 2014)

In this paper, we report on anisotropic transport properties of strained germanium (sGe) quantum wells grown on Si (001) substrates with p-type doping beneath the sGe channel. Mobility measurements were made along orthogonal [110] directions. The level of measured resistivity anisotropy in the [110] and [$\bar{1}$10] orientations was found to vary between 2 and 9 for different samples. This corresponds to an actual mobility anisotropy ratio of between 1.3 and 2, values that are significantly higher than previously found for sGe. From modeling of the low temperature (12 K) mobility, using the relaxation time approach, the anisotropy in mobility was accounted for by a difference in interface roughness scattering between the two orientations. For the [110] orientation, a step height of $\Delta = 0.28$ nm and interface roughness periodicity of $\lambda = 7$ nm were found while for the [$\bar{1}$10] orientation, λ reduced to 4 nm and Δ increased to 0.42 nm. High-resolution X-ray diffraction and transmission electron microscopy confirmed a 1° off-cut in the wafer towards the [$\bar{1}$10] direction.
© 2014 Author(s). All article content, except where otherwise noted, is licensed under a Creative Commons Attribution 3.0 Unported License. [http://dx.doi.org/10.1063/1.4870392]

Silicon remains the material of choice for many microelectronic applications because of its abundance and low cost, and in order to keep advancing this technology platform, innovative solutions such as the incorporation of other materials have been sought. To improve the hole mobility Ge has been adopted because not only is it fully miscible with silicon but it also has a higher hole mobility. Furthermore, through controlled epitaxial growth, the lattice mismatch between Si and Ge can be exploited to introduce strain to the active layer. The introduction of strain results in a splitting of the heavy and light hole bands, which in turn leads to a reduction in the hole effective mass and the interband scattering.[1] This has been shown to result in a further enhancement of the hole mobility,[2] thereby offering significant performance improvement over current Si-based device technology.[3] A common approach adopted for studying the transport properties of strained Ge (sGe) is through the epitaxial growth of a two-dimensional hole gas (2DHG) structure. Due to the large mismatch between Si and Ge (4.2%), a highly crystalline sGe layer of sufficient thickness to confine the carriers can only be realized if the sGe layer is grown on top of a Ge-rich $Si_{1-x}Ge_x$ buffer layer. For this work, we used a relaxed $Si_{0.2}Ge_{0.8}$ buffer for which the valance band offset to the strained Ge is about 100 meV,[1] making it comparable to the conduction band offset that was used in the strained silicon two-dimensional electron gas (2DEG)[4,5] structure that achieved a high electron mobility of 2×10^6 cm^2 V^{-1} s^{-1}.

Transport properties of sGe quantum wells (QWs) have been reported for a number of different growth methods, e.g., low-energy plasma-enhanced chemical vapor deposition (LEPE-CVD)[6–8] and molecular beam epitaxy (MBE).[9,10] From these growth methods, the highest low temperature Hall mobility for holes recorded was 1.2×10^5 cm^{-2} V^{-1} s^{-1} at 2 K,[8] while at room temperature it was 3100 cm^2 V^{-1} s^{-1}.[11] Recently, the growth of a sGe QW by reduced pressure chemical vapor deposition (RP-CVD)[12,13] has significantly improved on all previous results, with a hole Hall mobility of 1.1×10^6 cm^{-2} V^{-1} s^{-1} at a sheet density of 2.9×10^{11} cm^{-2} at 12 K reported for a "normal" structure (i.e., with doping above the channel). The main reasons given for the extremely high mobility found in this structure was the purity of the Ge channel (Si $<$ 0.01%) and the low level of background impurities in the channel.

In this paper, we report on a set of samples (11–284, 11–285, 11–286, 11–287, 11–288) that were grown at the same time and using the same system that produced the wafer (11–289) with the highest reported 2DHG mobility at low temperature.[12] However, a significant difference between these samples and that of Ref. 12 is that the doping was placed below the sGe QW channel, i.e., they are "inverted" structures. The samples were grown using an ASM Epsilon 2000 RP-CVD reactor and consisted of a 100 mm diameter Si (001) substrate (10–20 Ω cm) on top of which was deposited a 2.1 μm thick, relaxed $Si_{0.2}Ge_{0.8}$ reverse linearly graded (RLG) buffer.[14] This strain tuning buffer[15] is grown without any chemical mechanical polishing (CMP) and previously found to have a low threading dislocation density (TDD) of $\leq 4 \times 10^6$ cm^{-2}.[14,16] On top of the RLG buffer, a B-doped supply layer, an undoped $Si_{0.2}Ge_{0.8}$ spacer layer and then the sGe QW were grown, followed by another undoped $Si_{0.2}Ge_{0.8}$ layer and finally a thin Si cap. The Ge QW was confirmed to be fully strained for all the samples by high resolution X-ray diffraction (HR-XRD) reciprocal space mapping (strain is 0.65% ± 0.01%). The QW width, spacer layer thickness, and doping level were varied within the sample set as set out in Table I.

a)Also at Department of Physics, Tripoli University, Libya. Electronic addresses: amnahassan53@yahoo.co.uk, A.H.A.H.Hassan@warwick.co.uk.
b)Also at International Laboratory of High Magnetic Fields and Low Temperatures, Gajowicka 95, 53-421 Wroclaw, Poland. Electronic addresses: oamironov@yahoo.co.uk and O.A.Mironov@warwick.ac.uk.

 © Author(s) 2014

This article is copyrighted as indicated in the article. Reuse of AIP content is subject to the terms at: http://scitation.aip.org/termsconditions. Downloaded to IP: 137.205.202.72 On: Mon, 12 May 2014 12:15:48

TABLE I. Measured hole density (p_s) and mobility at 12 K, for both the $[\bar{1}10]$ and $[110]$ orientations, along with layer thicknesses taken from uleSIMS measurements (or XTEM where indicated).

Sample	Orientation	$p_s \times 10^{11}\,cm^{-2}$	Mobility $\times 10^5\,cm^2/V\,s$	Layer thickness (nm) Channel	Spacer	Doping layer	Doping density $\times 10^{17}\,cm^{-3}$
11–284	$[\bar{1}10]$	5.03	2.47	22 ± 2 (XTEM)	20 ± 2	18 ± 3	7 ± 3
	$[110]$		3.36				
11–285	$[\bar{1}10]$	6.90	2.74	15 ± 2 (XTEM)	26 ± 2	12 ± 3	9 ± 3
	$[110]$		3.57				
11–286	$[\bar{1}10]$	6.75	2.65	38 ± 2 (XTEM)	20 ± 2	21 ± 3	9 ± 3
	$[110]$		3.48				
11–287	$[\bar{1}10]$	7.89	1.12	22 ± 2	12 ± 2	19 ± 3	10 ± 3
	$[110]$		2.15				
11–288	$[\bar{1}10]$	6.51	1.77	20 ± 2	24 ± 2	15 ± 3	18 ± 3
	$[110]$		2.81				

The structural properties of all the samples were studied by ultra-low energy secondary ion mass spectrometry (uleSIMS) using a near normal incidence O_2^+ primary beam at 250 eV (Figure 1, typical profile), HR-XRD using a Panalytical X'Pert Pro MRD diffractometer equipped with a hybrid monochromator giving pure Cu $K_{\alpha 1}$ radiation in triple axis configuration, and cross-sectional transmission electron microscopy (XTEM) (Figure 2, typical image). All the layer thicknesses were determined by both XTEM and uleSIMS and found to be in excellent agreement while the average B doping concentration was obtained from uleSIMS. Table I summarizes all the values determined. The background B impurity levels elsewhere in the structure were below $10^{17}\,cm^{-3}$, as determined by the uleSIMS detection limit (From the previous SIMS measurements, with a lower noise floor, on material grown in this epitaxy system that used the same strain tuning buffer we believe the background impurity density to actually be below $10^{15}\,cm^{-3}$). Furthermore, the uleSIMS measurements also indicate that the Si concentration at the center of the sGe channel was in the range of 0.01–0.1 at. %, confirming that the low temperature (400 °C) epitaxy approach used here had achieved a high purity sGe channel with minimal Si penetration to the sGe channel. The quality of the sGe interfaces also showed minimal roughening (<1 nm) as indicated by the XTEM imaging and is best observed from the compressed version of the image shown on the right of Figure 2.

For the transport measurements, Van der Pauw (VdP) structures were produced using wet chemical etching. Al contacts were deposited on the corners of the square samples (4 × 4 mm) by thermal evaporation and then annealed at 425 °C for 20 min under dry N_2 to ensure ohmic behavior. Resistivity and Hall measurements were performed on all the samples over the temperature range of 12–300 K at a magnetic field of 0.6 T for current flow in the two perpendicular surface directions, i.e., $[110]$ and $[\bar{1}10]$, to study the anisotropy in the 2D-hole mobility

The ratio of resistances measured in perpendicular directions from a VdP sample overestimates the actual resistivity anisotropy for two reasons: first due to geometrical effects of the actual sample shape and positioning of the contacts and second, after correcting for geometry, an anisotropic resistance will alter the current flow and electric field distribution in the sample. The full analysis of this was provided by Bierwagen,[17] and also mentioned recently by Martin,[18] which allows us to convert the measured resistance ratio to a

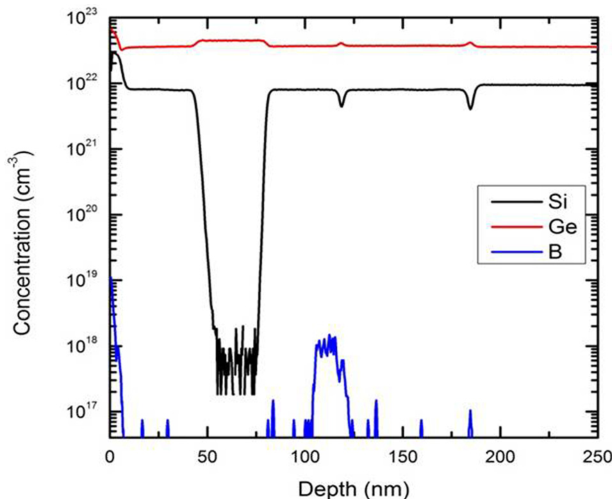

FIG. 1. uleSIMS depth profile showing the B, Si, and Ge distribution within sample 11–286.

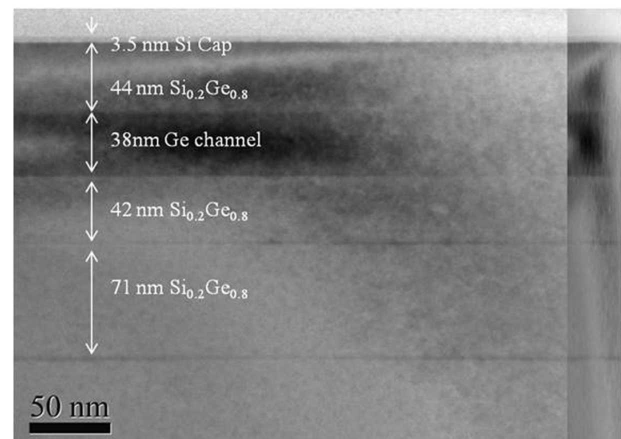

FIG. 2. XTEM image for the sample 11–286 with a 10× compression of the image on the right side to help show up any interface roughness.

This article is copyrighted as indicated in the article. Reuse of AIP content is subject to the terms at: http://scitation.aip.org/termsconditions. Downloaded to IP: 137.205.202.72 On: Mon, 12 May 2014 12:15:48

mobility anisotropy. The measured anisotropy ratio A_{VdP} is related to an effective resistance anisotropy A_{eff} by

$$A_{VdP} = \frac{\sum_{n=odd^+} \left[n \times \sinh\left(\sqrt{A_{eff}^{-1}} \pi n \right) \right]^{-1}}{\sum_{n=odd^+} \left[n \times \sinh\left(\sqrt{A_{eff}} \pi n \right) \right]^{-1}}. \quad (1)$$

For an anisotropy of less than 10, a satisfactory approximation can be obtained with just the $n=1$ terms and a look-up table to find A_{eff}. From this, the actual anisotropy coefficient A can be determined with a simple geometrical correction $A = A_{eff} \times (L_y/L_x)^2$, where L_y and L_x are the distances between contacts in the orthogonal directions. Finally, the resistivity for both orientations can be defined as $\rho_{xx} = \rho_{ave}\sqrt{A^{-1}}$, and $\rho_{yy} = \rho_{ave}\sqrt{A}$, and the mobility calculated using the measured Hall Coefficient. Table I summarizes the calculated 12 K VdP mobility and sheet density found for $[\bar{1}10]$ and $[110]$ orientations in all the samples.

Significant anisotropy is observed in the mobility for temperatures below 100 K. However, at higher temperatures (100–300 K) this anisotropy almost disappears ($\sim$1), although here parallel conduction dominates which may well mask any channel anisotropy that is not present in the parallel conduction layers. This was used as a check on the geometry of the samples; a correction was made for sample 11–288, but all the others had A(300 K) sufficiently close to unity that no adjustments were made. The ratio of calculated sheet resistivity between the two directions, i.e., $[110]$ and $[\bar{1}10]$ (Figure 3), is found to be of the order 1.3 for the samples 11–284, 11–285, and 11–286. For samples 11–288 and 11–287, this rises to 1.5 and 2, respectively, indicating a much stronger anisotropy in the sample which corresponds to the largest measured sheet density. For the asymmetric doping arrangement in our structures, Poissson-Schrödinger simulation of the electrostatics shows that the hole wavefunction is predominantly at the lower interface of the quantum well and this invariance of mobility suggests that even

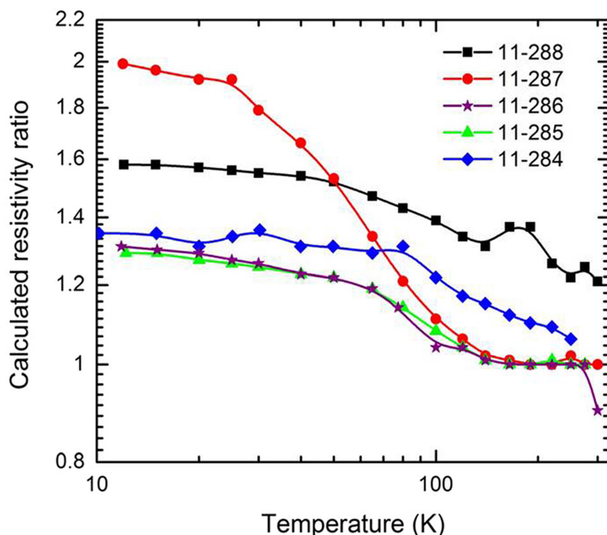

FIG. 3. Calculated resistivity ratio for the temperature range of 10 K–300 K for all samples and both orientations ($[\bar{1}10]$ and $[110]$).

for a 15 nm wide well the holes are not significantly affected by the other interface. We might expect that for thinner quantum wells there would be some reduction in mobility. For each sample, the same Hall coefficient value was observed for both orientations, which would be expected since the value of carrier density should be the same in whichever direction it is measured; however, this does confirm that the measured mobility anisotropy is a consequence of different scattering rates in the two directions.

There are a number of scattering mechanism contributing to the hole mobility. At high temperature, the dominant mechanism is expected to be phonon scattering,[19] which should be isotropic; indeed the measured difference in resistivity vanishes above about 200 K. Ionized impurity scattering is also isotropic; at low temperature and low carrier density, scattering from background impurities will be most important, with the influence of remote impurities (in the B-supply layer) increasing at higher hole density. The influence of interface roughness scattering also increases with carrier density,[20] and roughness can vary with orientation. It is therefore reasonable to investigate whether interface roughness scattering is responsible for the anisotropy that we see increasing with hole density. Indeed a previous study on GaAs (Ref. 21) did attribute a mobility anisotropy that increased with sheet density to interface roughness or substrate off-cut.[22–24] We have therefore calculated the mobility contributions from these various scattering mechanisms to compare with the experimental values. We used the relaxation time approach to calculate the remote impurity scattering rate as[25–28]

$$\frac{1}{\tau_{RI}} = \frac{e^4 m^* n_i}{8\pi\hbar^3 \varepsilon^2 q_F^3} \int_0^{\pi} \frac{e^{(-4q(L_s+w)\sin\theta)} \sin\theta}{(\sin\theta + S_0/2q_F)^2} d\theta, \quad (2)$$

where n_i is the remote ionized impurity density, e is the electron charge, m^* is the effective mass of the holes which is assumed to be isotropic in our samples because a similar level of strain was found for both orientations by HR-XRD. The effective mass value used in this study was 0.07 m_0 which had been extracted previously using magnetotransport measurements of 11–284,[13] q_F is the Fermi wave vector, L_s is the spacer thickness, w is the channel thickness, and S_0 is the screening constant.[26]

For background impurity scattering we have[27,28]

$$\frac{1}{\tau_{BI}} = \frac{e^4 m^* N_B}{8\pi\hbar^3 \varepsilon^2 q_F^2} \int_0^{\pi} \frac{\sin\theta(1 - e^{-2q_F\sin\theta})}{(\sin\theta + S_0/2q_F)^2} d\theta, \quad (3)$$

where N_B is the two-dimensional background impurity density in the QW.

Finally, the relaxation time for interface roughness scattering is given by[29]

$$\frac{1}{\tau_{IR}} = \frac{e^4 m^* \Delta^2 \Lambda^2}{\hbar^3 \varepsilon^2} \left(N_{Depl} + \frac{p_s}{2} \right)^2 e^{\frac{-q^2\Lambda^2}{4}}, \quad (4)$$

where the hole sheet density p_s and N_{Depl} determine the effective normal electric field in the channel. Δ parameterizes the interface roughness height, and Λ is the interface roughness correlation length, in the direction being

This article is copyrighted as indicated in the article. Reuse of AIP content is subject to the terms at: http://scitation.aip.org/termsconditions. Downloaded to IP: 137.205.202.72 On: Mon, 12 May 2014 12:15:48

considered. We note that, whilst Δ and Λ are related to physical dimensions in the sample, they are treated as variable parameters in the modeling.

Figure 4 shows the best agreement found with our calculated mobilities along with the parameters used to obtain this. According to our simulations, the best fit for both orientations was achieved for a remote ionized impurity level of $3 \times 10^{17}\,\text{cm}^{-3}$ and background impurity level of $2 \times 10^{14}\,\text{cm}^{-3}$. Although the latter is well below the SIMS detection threshold, it is a realistic value that is consistent with estimates of the residual impurity levels from, for instance, dark-count measurements in Ge detectors grown in the same system. It is also slightly greater than the value of $5 \times 10^{13}\,\text{cm}^{-3}$ that we needed to use in simulations[30] that reproduce the higher measured mobility in the normal structure of Ref. 12. In the $[110]$ orientation, an interface roughness height of $\Delta = 0.28\,\text{nm}$ with interface roughness periodicity $\Lambda = 7\,\text{nm}$ was found. For the $[\bar{1}10]$ orientation, the roughness height Δ increased to 0.42 nm and the correlation length Λ had to be reduced (4 nm). These findings indicate that the large mobility anisotropy observed arises from a monolayer roughness (up to ~3 monolayers) that has a nm-scale periodicity, possibly due to the (001) Si substrate off-cut leading to a step like structure for the $[\bar{1}10]$ direction.[22–24]

Although the initial XTEM measurements (shown in Figure 2) do not reveal any interface roughness in our structures, anything below about 1 nm would not be obvious in the images. Further high-resolution XTEM images were obtained using an aberration corrected microscope that do appear to show a significant difference in off-cut angle between the two orientations, i.e., $\langle 110 \rangle$ and $\langle \bar{1}10 \rangle$ of up to 1° (see Table II). (The values reported are averages of at least three measurements per sample direction with an uncertainty of ±0.3° coming from the spread in measured slopes.) The orientation of the wafers was also measured by HR-XRD. Accurate positions of the (224), (044), and (004) reflections were determined and hence the misorientation of the wafer relative to the goniometer could be found via an orientation matrix. This enabled the relative off-cut in $[110]$

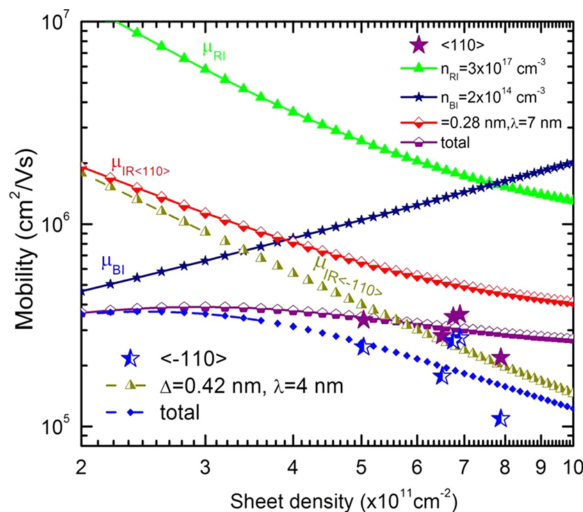

FIG. 4. Mobility simulation for the ($[\bar{1}10]$ and $[110]$) orientations taking into account remote impurity scattering, background impurity scattering, and interface roughness.

TABLE II. Substrate off-cut angle determined from XRD and HR-TEM for orthogonal directions.

Sample	Orientation	Si substrate off-cut angle (XRD)	Si substrate off-cut angle (XTEM)
11–287	$[\bar{1}10]$	1.1° ± 0.1°	1.5° ± 0.3°
11–287	$[110]$	0.1° ± 0.1°	0.3° ± 0.2°
11–288	$[\bar{1}10]$	1.0° ± 0.1°	0.9° ± 0.6°
11–288	$[110]$	0.2° ± 0.1°	0.4° ± 0.2°

and $[\bar{1}10]$ directions to be calculated to ±0.1 (Table II). Both measurement techniques agree that there is about a 1° off-cut towards $[\bar{1}10]$. This difference in off-cut angle will affect both the terrace height and length and hence the scattering rates in the two orthogonal directions.

In conclusion, significant mobility (resistivity) anisotropy between $[110]$ and $[\bar{1}10]$ orientations has been found in sGe quantum well structures. The anisotropy coefficient determined was between 1.3 and 2. Using the relaxation time approximation for isotropic remote impurity scattering, background impurity scattering, and anisotropic interface roughness scattering, it was found that the difference in mobility could be modeled by varying the interface roughening scattering parameters between the two orientations. For the $[110]$ direction, an interface roughness height of $\Delta = 0.28\,\text{nm}$ with interface roughness periodicity $\Lambda = 7\,\text{nm}$ was found but for the $[\bar{1}10]$ orientation a larger roughness height ($\Delta = 0.42\,\text{nm}$) and shorter periodicity ($\Lambda = 4\,\text{nm}$) were found, indicating a larger interface roughness effect was affecting the mobility in the $[\bar{1}10]$ direction. HR-XRD and XTEM results appear to indicate this interface roughness variation is from a 1° difference in off-cut angle between $[110]$ and $[\bar{1}10]$ orientations which may arise from the starting (001) Si substrate.

This work was partially supported by EPSRC projects EP/F031408/1 and EP/J001074/1; the Slovak Research and Development Agency under Contract Nos. APVV-0132-11 and VEGA-0106-13, and SAS Centre of Excellence CFNT MVEP (Kosice, Slovakia). OAM acknowledges the National Scholarship Program of the Slovak Republic for the Mobility Support for Researchers the Academic Year 2012/2013. The Panalytical MRD diffractometer used was obtained through the Science City Advanced Materials Project, with support from Advantage West Midlands and part funded by the European Regional Development Fund.

[1] F. Schaffler, Semicond. Sci. Technol. **12**(12), 1515–1549 (1997).
[2] K. Sawano, H. Satoh, Y. Kunishi, K. Nakagawa, and Y. Shiraki, Semicond. Sci. Technol. **22**(1), S161–S163 (2007).
[3] S. M. Sze, *Physics of Semiconductor Devices*, 2nd ed. (Wiley, New York, 1981).
[4] T. M. Lu, C.-H. Lee, S.-H. Huang, D. C. Tsui, and C. W. Liu, Appl. Phys. Lett. **99**(15), 153510 (2011).
[5] S.-H. Huang, T.-M. Lu, S.-C. Lu, C.-H. Lee, C. W. Liu and D. C. Tsui, Appl. Phys. Lett. **101**(4), 042111 (2012).
[6] H. von Kanel, D. Chrastina, B. Rossner, G. Isella, J. P. Hague, and M. Bollani, Microelectron. Eng. **76**(1-4), 279–284 (2004).
[7] H. von Kanel, M. Kummer, G. Isella, E. Muller, and T. Hackbarth, Appl. Phys. Lett. **80**(16), 2922–2924 (2002).

This article is copyrighted as indicated in the article. Reuse of AIP content is subject to the terms at: http://scitation.aip.org/termsconditions. Downloaded to IP: 137.205.202.72 On: Mon, 12 May 2014 12:15:48

[8]B. Rossner, D. Chrastina, G. Isella, and H. von Kanel, Appl. Phys. Lett. **84**(16), 3058–3060 (2004).
[9]T. Irisawa, H. Miura, T. Ueno, and Y. Shiraki, Jpn. J. Appl. Phys., Part 1 **40**(4B), 2694–2696 (2001).
[10]M. Myronov, T. Irisawa, O. A. Mironov, S. Koh, Y. Shiraki, T. E. Whall, and E. H. C. Parker, Appl. Phys. Lett. **80**(17), 3117–3119 (2002).
[11]M. Myronov, K. Sawano, Y. Shiraki, T. Mouri, and K. M. Itoh, Appl. Phys. Lett. **91**(8), 082108 (2007).
[12]A. Dobbie, M. Myronov, R. J. H. Morris, A. H. A. Hassan, M. J. Prest, V. A. Shah, E. H. C. Parker, T. E. Whall, and D. R. Leadley, Appl. Phys. Lett. **101**(17), 172108 (2012).
[13]A. H. A. Hassan, O. A. Mironov, A. Feher, E. Cizmar, S. Gabani, R. J. H. Morris, A. Dobbie, V. A. Shah, M. Myronov, L. B. Berkutoy, V. V. Andrieyskii, and D. R. Leadley, in International Conference on Ultimate Integration on Silicon (ULIS-14), Warwick, March 2013.
[14]V. A. Shah, A. Dobbie, M. Myronov, D. J. F. Fulgoni, L. J. Nash, and D. R. Leadley, Appl. Phys. Lett. **93**(19), 192103 (2008).
[15]M. Myronov, A. Dobbie, V. A. Shah, X. C. Liu, V. H. Nguyen, and D. R. Leadley, Electrochem. Solid State Lett. **13**(11), H388–H390 (2010).
[16]V. A. Shah, A. Dobbie, M. Myronov, and D. R. Leadley, J. Appl. Phys. **107**(6), 064304 (2010).
[17]O. Bierwagen, R. Pomraenke, S. Eilers, and W. T. Masselink, Phys. Rev. B **70**(16), 165307 (2004).
[18]N. Martin, J. Sauget, and T. Nyberg, Mater. Lett. **105**(0), 20–23 (2013).
[19]A. M. Savin, C. B. Soerensen, O. P. Hansen, N. Y. Minina, and M. Henini, Semicond. Sci. Technol. **14**(7), 632 (1999).
[20]T. Ando, A. B. Fowler, and F. Stern, Rev. Mod. Phys. **54**(2), 437–672 (1982).
[21]Y. Markus, U. Meirav, H. Shtrikman, and B. Laikhtman, Semicond. Sci. Technol. **9**(7), 1297 (1994).
[22]R. Neumann, K. Brunner, and G. Abstreiter, Physica E **13**(2–4), 986–989 (2002).
[23]R. Neumann, J. Zhu, K. Brunner, and G. Abstreiter, Thin Solid Films **380**(1–2), 124–126 (2000).
[24]H. Lichtenberger, M. Mühlberger, C. Schelling, and F. Schäffler, J. Cryst. Growth **278**(1–4), 78–82 (2005).
[25]C. J. Emeleus, T. E. Whall, D. W. Smith, R. A. Kubiak, E. H. C. Parker, and M. J. Kearney, J. Appl. Phys. **73**(8), 3852–3856 (1993).
[26]K. Lee, M. S. Shur, T. J. Drummond, and H. Morkoc, J. Appl. Phys. **54**(11), 6432–6438 (1983).
[27]J. Lee, H. N. Spector, and V. K. Arora, J. Appl. Phys. **54**(12), 6995–7004 (1983).
[28]K. Hess, Appl. Phys. Lett. **35**(7), 484–486 (1979).
[29]D. Monroe, Y. H. Xie, E. A. Fitzgerald, P. J. Silverman, and G. P. Watson, J. Vac. Sci. Technol., B **11**(4), 1731–1737 (1993).
[30]A. H. A. Hassan, "Transport properties for pure strained Ge quantum well," Ph.D. thesis, University of Warwick, 2014.

This article is copyrighted as indicated in the article. Reuse of AIP content is subject to the terms at: http://scitation.aip.org/termsconditions. Downloaded to IP: 137.205.202.72 On: Mon, 12 May 2014 12:15:48